Vietnam Journal of Science and Technology ***63*** *(6) (2025) 1137-1146*

doi:10.15625/2525-2518/19189

Investigation of the formation of Cu_4SnS_4 using mechanical alloying and heat-treatment for thermoelectric conversion

Le Van Dai, Nguyen Tien Anh, Nguyen Thi Kieu Oanh, Le Thi Bang, Bui Duc Long*

School of Materials Science and Engineering, Hanoi University of Science and Technology, No. 1 Dai Co Viet, Bạch Mai, Ha Noi, Viet Nam

*Email: *long.buiduc@hust.edu.vn*

Received: 16 October 2023; Accepted for publication: 4 May 2024

Abstract. In this research, the Cu_4SnS_4 was synthesized using mechanical alloying method from Cu, Sn and S powders for different milling durations (0, 8, 16, and 20 hours) in high purity Ar atmosphere. As the results, the particle sizes of milled powders were rapidly decreased after 8 h milling and slightly decreased with further increasing in milling duration up to 16 hours and 20 hours. The Cu_3SnS_4 began to form after milling for 8 hours and completed its formation at 16 hours. With prolonged milling duration to 20 hours, it was still not possible to detect any trace for the formation of Cu_4SnS_4. After subsequent heat-treatment at 673 K, the Cu_3SnS_4 phase of 16 h-milling powder was completely converted to Cu_4SnS_4. The electrical conductivity (σ), Seebeck coefficient and power factor *(PF)* of sintered Cu_4SnS_4 sample increased with the increase of measured temperature, reaching maximum values of 1207 S m^{-1}, 250 μV K^{-1} and 75.5 μW K^{-2} m^{-1} at 723 K, respectively.

Keywords: Thermoelectric materials, Chalcogenide, Cu_4SnS_4, Synthesis, Spark plasma sintering.

Classification numbers: 2.8.2, 2.10.2.

1. INTRODUCTION

Energy and the environment pose the significant challenges in the 21st century [1]. The increase of population and manufacturing has resulted in increased energy demand, in particularly large developing countries such as BRICS. However, fossil fuels remain the primary energy resources at the present. The use of fossil fuels, such as natural gas, oil, and coal, has resulted in serious pollution and affect people's living environment. In addition, the used energy efficiency remains low, with statistics indicating that more than 60 % of the primary energy is wasted in the form of heat. Therefore, governments have been investing in green technologies to replace traditional energy resources with clean, renewable and sustainable resources such as solar, wind, ocean, and geothermal energies, while also focusing on improving energy efficiency [2 - 7].

Thermoelectricity (TE) offers a sustainable mean to recover and directly convert waste heat into usable electrical energy based on the Seebeck effect. This conversion technique enables power generation using waste heat (from processes in industrial production, vehicle exhaust, industrial electronic devices, combustion of solid waste, the human body etc.), and other

resources such as solar, geothermal energy [1, 8]. For example, BMW and Ford are well-known commercial vehicle companies, and a thermoelectric generator (TEG) built by Amerigon was attached to the exhaust gas pipe in their vehicles and produced around 500 W of electricity from the waste heat [9]. Nesrine *et al*. [10] reported that TEG can also generate electric power in the range of μW to mW from the low waste heat in our body to supply wearable devices such as watches, biomedical hearing aids etc.

The performance of a TE material is determined by the dimensionless figure of merit, $ZT = S^2\sigma T\kappa^{-1}$, where S is the Seebeck coefficient, σ is the electrical conductivity, T is the absolute temperature, and κ is the thermal conductivity [10]. For high efficiency conversion, a large power factor, $PF = S^2\sigma$, and a low κ value should be achieved [11]. Currently, the commercialization or large-scale production of thermoelectric devices are still limited by three main challenges, i.e., high cost elements and toxic constituents, and low efficiency [12]. Thus, a suitable approach needs to be developed.

In recent years, Cu–S based minerals appeared as potential candidates for TE conversion due to advantages, such as being earth abundant, low cost and less toxic constituent elements, e.g., Cu_2ZnSnS_4 (CZTS), Cu_4SnS_4, $CuFeS_2$, and $Cu_{1.8}S$, etc. [13 - 16]. Among these materials, the *p*-type Cu_4SnS_4 semiconductor was emerging as a potential TE material because of its low κ, relatively high S, and suitable bandgap of 0.9 - 1.7 eV [17]. The synthesis of Cu_4SnS_4 was mostly conducted by melting method [14,18,19]. However, this method has some disadvantages such as high temperature and long duration for homogenization process etc. According to Amitave *et al*. [15] the process of Cu_4SnS_4 synthesis was taken more than 295 hours. In contrast, powder metallurgy (P/M), in particular mechanical alloying method is a solid-state milling and reaction from constituent powders, which is able to overcome the limitations of the melting method [20].

In this research, the synthesis of Cu_4SnS_4 was used of mechanical alloying method from Cu, Sn, and S powders, followed by a short heat-treatment process. The phase evolution and particle sizes distribution were investigated for different milling duration samples. The phase transformation from Cu_3SnS_4 to Cu_4SnS_4 was investigated for the powder samples milled for 16 hours and heat-treated at temperatures of 673 and 873 K. The 16 h-milling powder was sintered using spark plasma sintering (SPS) for investigation of TE properties. i.e., the electrical conductivity (σ), Seebeck coefficient (S), and power factor (PF).

2. MATERIALS AND METHODS

2.1. Materials

Cu (99.5 %, -100 mesh, Strem Chemicals), Sn (99.5 %, -100 mesh, Alfa Aesar) and S (99.5 %, -325 mesh, Alfa Aesar) powders were used as starting materials. A mixture of the Cu, Sn and S powders was prepared at a stoichiometric ratio of 4 : 1: 4 in order to form Cu_4SnS_4. The entire powders preparation process was carried out in a glove box with a protective atmosphere of Ar gas.

2.2. Synthesis process

The mixed powders were milled for different duration of 0 hour, 8 hours, 16 hours, and 20 hours in Ar atmosphere using a Fritsch Planetary Mono Mill Pulverisette 6. The balls-to-powder ratio and rotation speed was set at 10 : 1 and 300 rpm, respectively. In order to avoid contamination from the milling process, a zirconia container and balls were used.

After milling, the Cu_4SnS_4 powders were heat-treated using a muffle furnace (Nabertherm B150) at temperatures of 673 K and 873 K for 1 hour under an Ar atmosphere. The heat-treated milled powders were consolidated using Spark Plasma Sintering (SPS) at 873 K under an applied pressure of 50 MPa for 15 minutes.

2.3. Characterization

The phase transformations after ball milling and heat treatment were analyzed by X-ray diffraction (XRD) using a Bruker D8 Advance diffractometer with Cu Kα radiation (1.54059 Å). The surface morphologies of the mixed and milled powders were observed by field emission-scanning electron microscopy (FE-SEM, Hitachi S4800). The particle size was measured from SEM images, with at least 50 particles using ImageJ software. The SPS samples were cut into the rectangular shape with sizes of 3 mm × 3 mm × 12 mm to measure the Seebeck coefficient and electrical conductivity, which used Linseis LSR-3 (Germani) equipment with a measured temperature range of 300 - 723 K under the He gas protective environment.

3. RESULTS AND DISCUSSION

3.1. Effect of milling duration on the morphology and particle sizes of milled powders

Secondary electron images (SEI) of the mixed Cu, Sn, and S powders for different milling duration of 0 hour, 8 hours, 16 hours and 20 hours are given in Fig. 1. The original mixture of powders exhibits the differences in shapes and sizes. The coarse particles are Cu powders with a porous structure, while Sn powders have a round shape, and S powders have an irregular shape (Fig. 1a). After milling for 8 hours, 16 hours and 20 hours, the mixture of Cu, Sn, and S powders became much finer and rounder, which was not able to distinguish the individual elements.

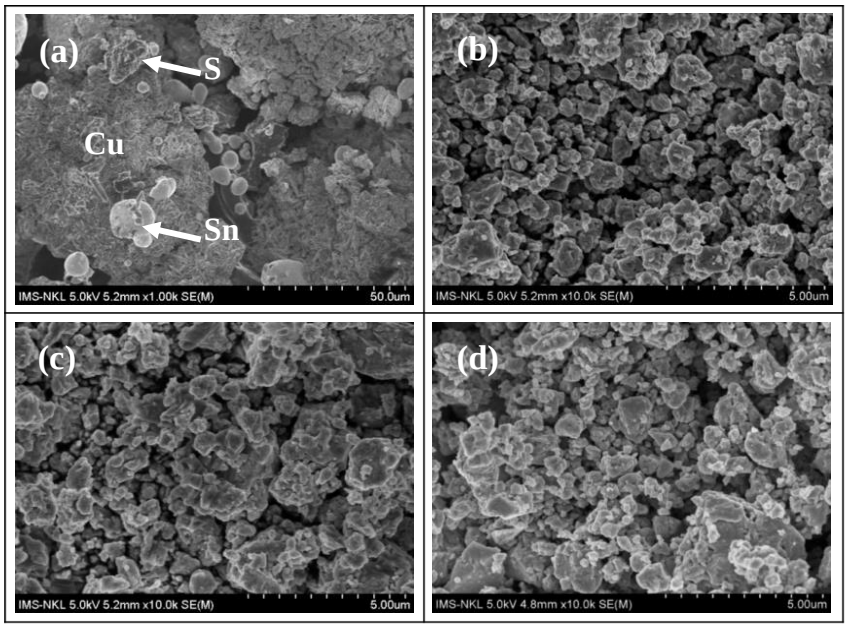

Figure 1. Secondary electron image (SEI) of the mixed Cu, Sn, and S powders for different milling duration (a) 0 h (b) 8 hours (c) 16 hours, and (d) 20 hours.

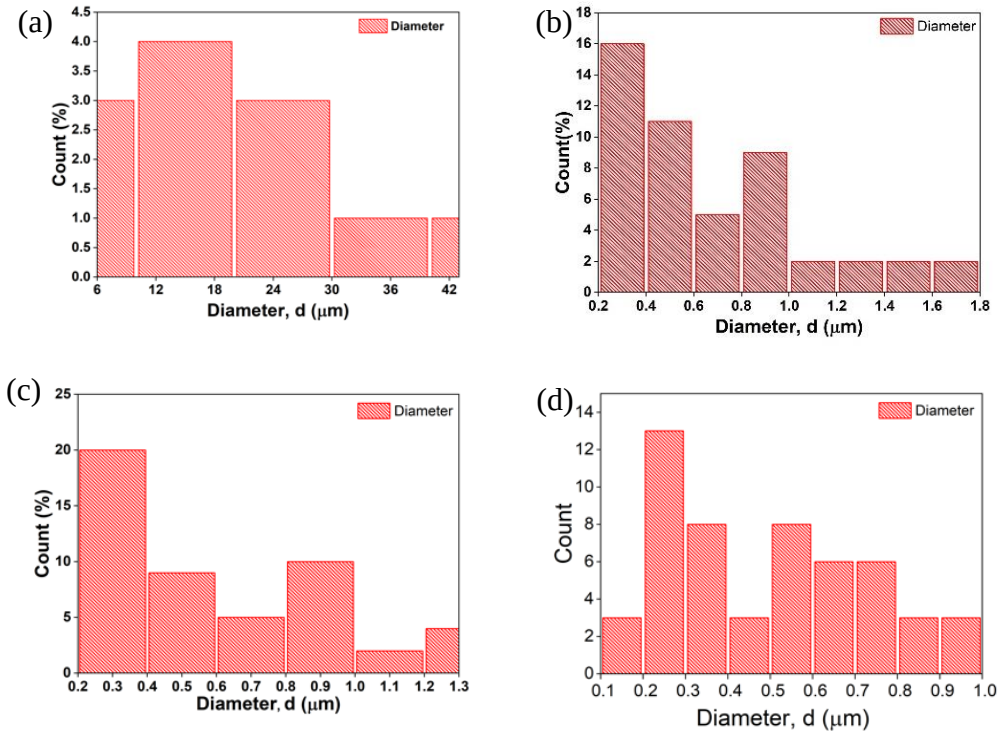

Figure 2. The particle size distributions of the mixed Cu, Sn, and S powders for different milling duration of (a) 0 hour, (b) 8 hours, (c) 16 hours, and (c) 20 hours.

The particle size distribution of the mixed Cu, Sn, and S powders for different milling duration are shown in Fig. 2, which indicated that the particle sizes of originally mixed powders ranged from 6 to 42 μm, with the majority falling in 12 - 18 μm (Fig. 2a). After 8 hour - milling, the particle sizes rapidly decreased to 0.2 - 1.8 μm, with a predominant distribution from 0.2 - 0.4 μm (Fig. 2b). The particle sizes further reduced to 0.2 - 1.3 μm after 16 hour - milling, and mainly distributed from 0.2 - 1.0 μm (Fig. 2c). After 20 hour - milling, the particle sizes reached their finest at about 0.1 - 1 μm, with the main distribution ranging from 0.2 - 0.8 μm (Fig. 2d).

It is evident that the average particle size of mixed powders decreased with increasing milling duration. It decreased from 18 μm to 0.63, 0.57 and 0.52 μm after milling for 0 h to 8 hours, 16 hours and 20 hours, respectively, as shown in Table 1. The initial milling stage, especially at 8 hours of milling, the average particle sizes of milled powders rapidly decreased from 18 μm to 0.63 μm. This can be attributed to the presence of S powder, which prevented the cold-welding process, as the results fracturing was dominant process. However, further increasing in milling duration to 16 hours and 20 hours, the milled particle powders slightly reduced, which could be explained due by the tendency of fine particles to agglomerate into larger ones, thereby reducing the refining efficiency [21].

To evaluate the refining efficiency of milling, the percentage of particle size reduction was calculated based on the difference between two consecutive milling duration intervals, as shown in Table 1. It can see that the percentage particle size reduction of the 8 hour-milling sample was of 96.5 %, whereas for the 16-hour and 20-hour milling samples were approximately 10.4 and 7.5 %, respectively. These results indicate a slight reduction in particle sizes after a prolonged milling duration.

Table 1. The average particle sizes and percentage of particle reduction of the mixed Cu, Sn, and S powders for different milling duration.

Milling duration (h)	Average particle size (μm)	Particle size reduction (%)
0	18	
8	0.63	96.5
16	0.57	10.4
20	0.52	7.5

3.2. Effect of milling duration on the phase formation

The XRD results of the mixed Cu, Sn, and S powders for different milling duration of 0 h, 8 hours, 16 hours and 20 hours are shown in Fig. 3. In the XRD pattern of the mixed powders (0 hour), all the peaks corresponded to the Cu, Sn and S elements. After milling for 8 hours, Cu_3SnS_4 began to form, but the XRD pattern still showed the presence of a low peak of a starting element, i.e. Sn. From the SEM image of the 8 hour-milling sample (Fig. 1b), it can be seen that the reaction was taking place when the element powders were well mixed and dissolved in each other, which were not able to observe by SEM. After increasing the milling duration to 16 hours, all the XRD peaks of starting elements were disappeared, while only the XRD peaks of the Cu_3SnS_4 phase existed. This result indicates the completed reaction between Cu, Sn and S powders to form Cu_3SnS_4. With further increasing milling duration to 20 hours, the XRD results showed only the existence of the Cu_3SnS_4 phase without any phase transformation or the formation of Cu_4SnS_4. Maheskumar [22] reported that the formation of Cu_3SnS_4 after 20 hours of milling of Cu, Sn, and S powders, with the reaction completed after 60 hours milling. However, they did not provide details on the apparatus and milling condition used in their research. Thus, we suggest that a heat-treatment process should be conducted on the milled powders to facilitate the formation of Cu_4SnS_4 from the milled powder, rather than further increasing the milling duration. Therefore, we chose the 16-hour-milling Cu_3SnS_4 powder for further study.

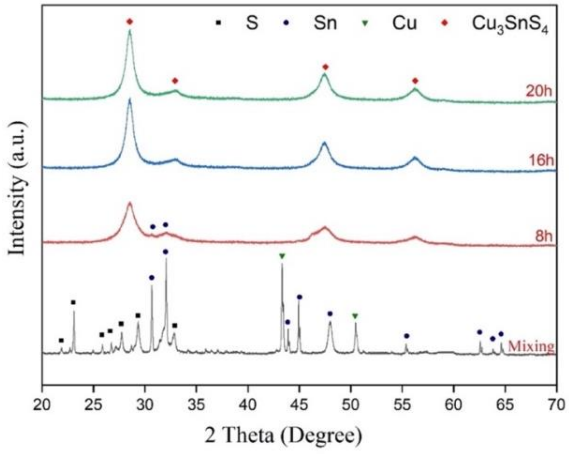

Figure 3. XRD patterns of the mixed Cu, Sn, and S powders milling for different duration.

The formation of Cu_3SnS_4 from Cu, Sn and S during mechanical milling can be explained by transferring the mechanical energy to the mixed powders during milling under collisions between the balls and between the balls and the wall of the milling container. After a certain

milling duration, the powders were well mixed and the particle sizes reduced, consequently reducing the diffusion distance between particle powders, which led to activate the reaction between the constituents [23, 24].

3.3. Effect of heat-treatment on phase transformation

Based on the DSC/TG results, the 16-hour-milled powders were subjected to heat treatment at 673 and 873 K to investigate the formation of Cu_4SnS_4. As shown in Fig. 4, the Cu_3SnS_4 phase was completely transformed into Cu_4SnS_4 phase after heat treatment at 673 K for 1 hour. Furthermore, upon increasing the heat-treatment temperature to 873 K, the XRD pattern still exhibited the presence of the single Cu_4SnS_4 phase. This transformation indicates that the formation of Cu_4SnS_4 can be simply achieved through a combination of mechanical alloying and heat-treatment process.

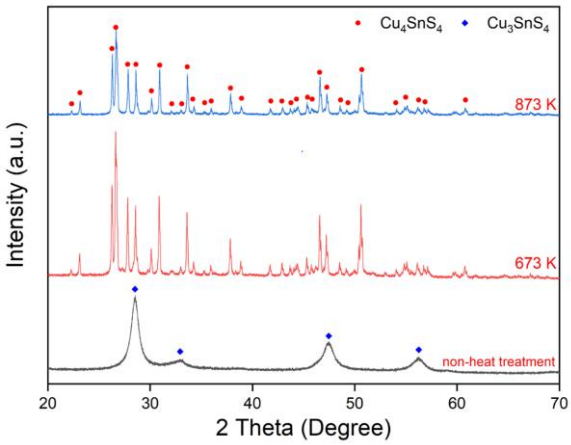

Figure 4. XRD patterns of heat-treated 16-hour-milling powders at different temperatures of 673 K and 873 K, and the non-heat treatment milled powder for the reference.

3.4 TE properties of sintered 16-hour milled Cu_4SnS_4

The TE properties of the sintered Cu_4SnS_4 sample, including the electrical conductivity, σ, and the Seebeck coefficient, S as well as the power factor, PF, were characterized in the temperature range of 300 - 723 K, as shown in Fig. 5.

The σ value sharply increased from 144.187 S m^{-1} at 303 K to 1207 S m^{-1} at 723 K, as shown in Fig. 5a, indicating that Cu_4SnS_4 is a semiconductor. The increase of σ value can be contributed to the increase of charge carrier's concentration, which results from the thermal excitation of electrons from the valence band to the conduction band when heat energy was applied [10,12, 25]. In this study, the σ value of pristine Cu_4SnS_4 is comparable to that of other Cu-based sulfides such as Cu_2ZnSnS_4 [12,20,26] and Cu_2SnS_3 [27]. However, this σ value is lower than that of Cu_3SnS_4, which exhibited metallic behavior. To enhance the performance of Cu_4SnS_4, further improvement of the σ value is required by increasing the carrier concentration [12, 26].

The S value of Cu_4SnS_4 sample also exhibited a sharp increase, rising from 127 μVK^{-1} at room temperature to 250 μVK^{-1} at 723 K, as shown in Fig. 5b. The positive S and the simultaneous increase of σ value with the temperature indicate that Cu_4SnS_4 is a *p*-type

semiconductor with holes as the major charge carriers [12, 13, 15]. This *S* value is relatively high and comparable to other TE materials such as Cu_2ZnSnS_4 [12, 26] and Cu_5FeS_5 [28].

The power factor (*PF*) was determined by using measured data from the σ and *S*, in which $PF = \sigma \times S^2$ (Fig. 5c). An increase in the value of $S^2\sigma$ was observed, rising from 2.3 $\mu WK^{-2}m^{-1}$ at 303 K to 75.5 $\mu WK^{-2}m^{-1}$ at 723 K. This resulted from the simultaneous increase in σ and *S*.

For comparison, the electrical conductivity, Seebeck coefficient, and power factor of Cu_4SnS_4 and other ternary Cu-based sulfides are given in Table 2. The σ of Cu_4SnS_4 is significantly higher than that of Cu_2SnS_3 [29], leading to correspondingly higher *PF*. However, its σ remains much lower than that of Cu_3SnS_4 [30] and Cu_5FeS_4 [28], resulting in a reduced the *PF*. Therefore, a further research work should focus on enhancing the σ of Cu_4SnS_4.

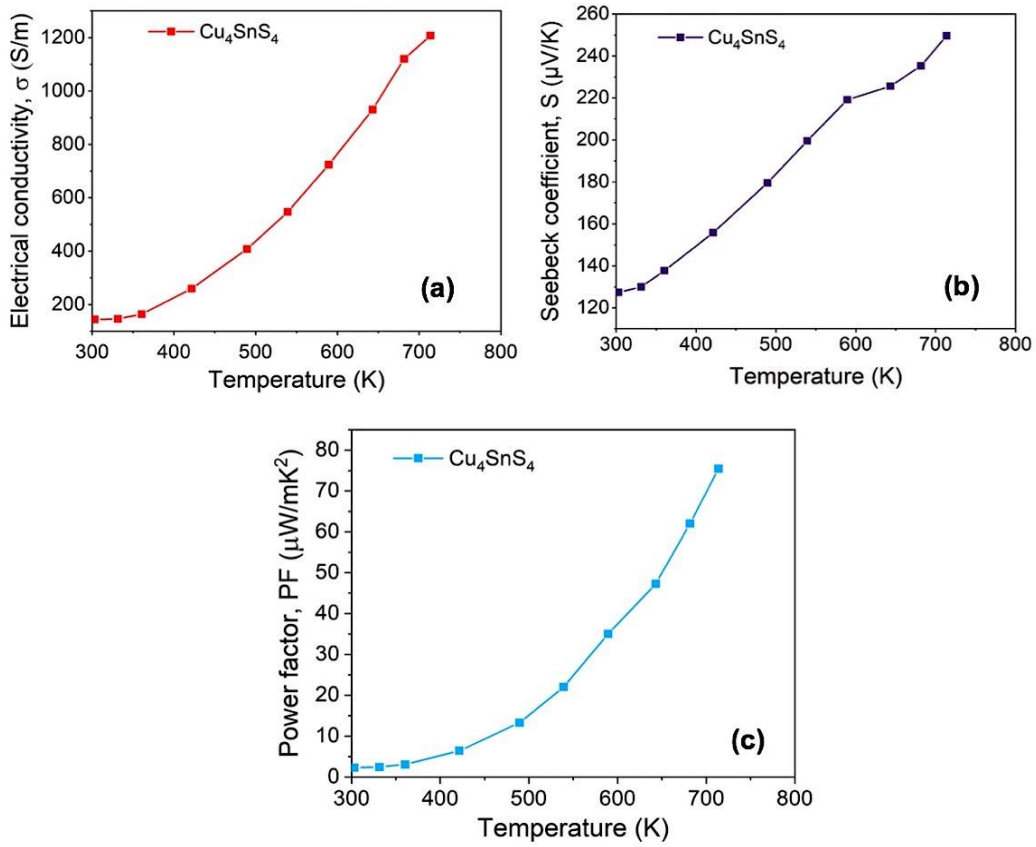

Figure 5. The TE properties of Cu_4SnS_4 after SPS at 873 K: (a) electrical conductivity (σ), (b) Seebeck coefficient (*S*), and (c) power factor (*PF*).

Table 2. Thermoelectric properties of Cu_4SnS_4 and other ternary Cu-based sulfides.

Sample	σ (S/m)	*S* μV/K	*PF* $\mu W/mK^2$	Measured temperature	Reference
Cu_4SnS_4	1207	250	75.5	723 K	Current work
Cu_2SnS_3	297	410	49.9	723 K	[29]
Cu_3SnS_4	1.3×10^5	103	1379.1	790 K	[30]
Cu_5FeS_4	2×10^4	155	480.5	710 K	[28]

4. CONCLUSIONS

This study investigated the synthesis of Cu_4SnS_4 using the mechanical alloying method from Cu, Sn, and S powders, combined with a heat-treatment process. The particle sizes of milled powders decreased with the increase of milling duration. The finest milled particle sizes were obtained for the 20 hour-milling sample, which mostly distributed in the range of 0.2 - 0.8 μm. Cu_3SnS_3 started to form after 8 hours of milling and completing at 16 hours of milling in a high-purity Ar atmosphere. Prolonged milling duration to 20 hours did not result in the formation of Cu_4SnS_4. Cu_3SnS_3 transformed into Cu_4SnS_4 after heat-treatment at 673 K for 1 hour. The electrical conductivity, Seebeck coefficient and power factor (PF) of sintered Cu_4SnS_4 sample increased with the measured temperature, reaching maximum values of 1207 Sm^{-1}, 250 μVK^{-1} and 75.5 $\mu WK^{-2}m^{-1}$ at 723 K, respectively.

Acknowledgements. This research is funded by Hanoi University of Science and Engineering (HUST) under project number T2022-PC-082.

CRediT authorship contribution statement. Le Van Dai: Methodology, Investigation. Nguyen Tien Anh: Methodology, Investigation. Nguyen Thi Kieu Oanh: Methodology, Investigation. Le Thi Bang: Analysis, Editing. Bui Duc Long: Formal analysis, Supervision, Funding acquisition.

Declaration of competing interest. The authors declare that they have no known competing financial interests or personal relationships that could have appeared to influence the work reported in this paper.

REFERENCES

1. Fitriani, Ovik R., Long B. D., Barma M.C., Riaz M., Sabri M.F.M., Said S.M., Saidur R. - A review on nanostructures of high-temperature thermoelectric materials for waste heat recovery, Renew. Sust. Energ. Rev. **64** (2016) 635-659. https://doi.org/10.1016/j.rser.2016.06.035.
2. Zeb K., Ali S.M., Khan B., Mehmood C.A., Tareen N., Din W., Farid U., Haider A. - A servey on weast heat recovery: Electricpower generation and potential prospects within Pakistan, Renew. Sust. Energ. Rev. **75** (2017) 1142-1155. https://doi.org/10.1016/j.rser.2016.11.096.
3. Xiao Z., Li-D. Z. - Thermoelectric materials: Energy conversion between heat and electricity, J. Materiomics **1** (2015) 92-105. http://dx.doi.org/10.1016/j.jmat.2015.01.001.
4. Cátia R.S. R., Telmo M., Ana L. P., Benedita C., Francisco S. C., André M. P. - Recovery of thermal energy released in the composting process and their conversion into electricity utilizing thermoelectric generators, Appl. Therm. Eng. **138** (2018) 319–324. https://doi.org/10.1016/j.applthermaleng.2018.04.046.
5. Yulong Zh., Wenjie L., Xianglin Zh., Yulin W., Ding L., Yanzhe L., Minghu G. - Energy and exergy analysis of a thermoelectric generator system for automotive exhaust waste heat recovery, Appl.Therm. Eng. **239** (2024) 122180. https://doi.org/10.1016/j.applthermaleng.2023.122180.
6. Yuncheng L., Junhui L., Lianbo M., Suilin W., Huixing Zh. - Waste heat recovery from exhausted gas of a proton exchange membrane fuel cell to produce hydrogen using thermoelectric generator, Appl. Energy **334** (2023) 120687. https://doi.org/10.1016/j.apenergy.2023.120687.

7. Yasin Ö., Emrah D. - Solar thermal waste heat energy recovery in solar distillation systems by using thermoelectric generators, Eng. Sci. Technol. Intern. J. **40** (2023) 101362.
8. Martin J.,Tritt, T., Uher C. - High temperature Seebeck coefficient metrology, J. Appl. Phys. **108** (2010) 121101. http://doi.org/10.1063/1.3503505.
9. Vladimir J. - Thermoelectric Waste Heat Recovery Program for Passenger Vehicles, U. S. Department of Energy 18 (2016).
10. Nesrine J., Ayda B., Jens M., Brahim M., Fares T., Mohammed I. - A comprehensive review of Thermoelectric Generators: Technologies and common applications, Energy Rep. **6**(7) (2020) 264-287. https://doi.org/10.1016/j.egyr.2019.12.011
11. Chang L., Fengxing J., Congcong L., Peipei L., Jingkun X. - Present and future thermoelectric materials toward wearable energy harvesting, Appl. Mater. Today **15** (2019) 543-557. https://doi.org/10.1016/j.apmt.2019.04.007.
12. Bui D. L., Le Hong T, Nguyen H. H., Koichiro S., Katsuaki H., Tran Q. M. N., Wojciech K., Michitaka O. - Thermoelectric quaternary sulfide $Cu_{2+x}Zn_{1-x}SnS_4$ (x = 0–0.3): Effects of Cu substitution for Zn, Mater. Sci. Eng. B **272** (2021) 115353. https://doi.org/10.1016/j.mseb.2021.115353.
13. Mohammad H., Kasim R., Mulla R. - Copper Sulfides: Earth Abundant and Low-Cost Thermoelectric Materials, Energy Technol. **7** (7) (2018) 1800850. http://doi.org/ 10.1002/ente.201800850.
14. Koichiro S., and Toshiro T. - Cu-S based synthetic minerals as efficient thermoelectric materials at medium temperatures, APL Mater. **4**(10) (2016) 104503. http://doi.org/10.1063/1.4955398.
15. Amitava C., Sudip M., Hooman Y., Seng H.L., Yew S. H., et al. - New insights into the structure, chemistry, and properties of Cu_4SnS_4, J. Solid State Chem. **253** (2017) 192-201. https://doi.org/10.1016/j.jssc.2017.05.033.
16. Abdul B., Jiwu X., Murtaza G., Lei W., Abdul H., Wang G., Jiyan Y. D. - Recent advances, challenges, and perspective of copper-based liquid-like thermoelectric chalcogenides: A review, Eco Mat. (2023) 5:e12391, https://doi.org/10.1002/eom2.12391.
17. Vasudeva R. M. R., Mohan R. P., Phaneendra R. G., Sreedevi G., Kishore Kumar Yarragudi B. R., Review on Cu_2SnS_3, Cu_3SnS_4, and Cu_4SnS_4 thin films and their photovoltaic performance, J. Ind. Eng. Chem. **67** (2019) 39-74. https://doi.org/ 10.1016/j.jiec.2019.03.035
18. Fiechter S., Martinez M., Schmidt G., Henrion W., Tomm Y. - Phase relations and optical properties of semiconducting ternary sulfides in the system Cu–Sn–S, J. Phys. **64** (2003) 1859-1862.
19. Akitoshi S., Naoyuki N., Youhei K., Masaki Wa., Takuji K., Ryoji A. - Presence of a Doubly-Splitting Site and Its Effect on Thermoelectric Properties of Cu_4SnS_4, Mater. Trans. **56** (6) (2015) 858-863. doi:10.2320/matertrans.E-M2015804.
20. Bui D. L., Nguyen V. K., Duong N. B., Nguyen H. H., Thermoelectric properties of quaternary chalcogenide Cu_2ZnSnS_4 synthesised by mechanical alloying, Powder Metall **63** (2020) 220-226. https://doi.org/10.1080/00325899.2020.1783103.
21. Suryanarayana C. - Mechanical alloying and milling, Prog. Mater. Sci. **46** (2001) 1-184.

22. Maheskumar V., Balaji G., Vidhya B. - Investigations on the structural, optical and visible light photocatalytic activity of Cu_3SnS_4 prepared by mechanical alloying, J. Mater .Sci. Mater. Electron. **28** (2017) 19081-19089. DOI 10.1007/s10854-017-7862-x.
23. Laszlo T. - Self-sustaining reactions induced by ball milling, Prog. Mater. Sci. **47** (2002) 355-414.
24. Long B. D., Zuhailawati H., Umemoto M., Todaka Y., Othman R. - Effect of ethanol on the formation and properties of a Cu–NbC composite, J. Alloys Compd. **503** (2010) 228-232. doi:10.1016/j.jallcom.2010.04.243.
25. William D. C. Jr., David G. R. - Materials Science and Engineering an Introduction, 8th edition, John Wiley & Sons Inc, 2009.
26. Min L. L., Fu Q. H., Li D. Chen., I-Wei C. - A wide-band-gap p-type thermoelectric material based on quaternary chalcogenides of Cu_2ZnSnQ_4 „Q = S, Se…, Appl. Phys. Lett. **94** (2009) 202103. DOI: 10.1063/1.3130718.
27. Zhen Zh., Huiwen Zh., Yifeng W., Xiaohui H., Yinong L., Changchun Ch, Lin P, Chunhua L. - Role of crystal transformation on the enhanced thermoelectric performance in Mndoped Cu_2SnS_3, J. Alloys. Coumpd. **780** (2019) 618-625. https://doi.org/10.1016/j.jallcom.2018.11.329
28. Aijuan Zh., Bin Zh., Wei L., Dandan X., Hongxia O., Xiaodong H., Jiyan D., Xu L., Guang H., Guoyu W., Xiaoyuan Zh. - Twin Engineering in Solution-Synthesized Nonstoichiometric Cu_5FeS_4 Icosahedral Nanoparticles for Enhanced Thermoelectric Performance, Adv. Funct. Mater. 2018, 1705117. DOI: 10.1002/adfm.201705117.
29. Yawei Sh., Chao L., Rong H., Ruoming T., Yang Y., Lin P., Kunihito K., Ruizhi Zh., Chunlei W., Yifeng W. - Eco-friendly p-type Cu_2SnS_3 thermoelectric material: crystal structure and transport properties, Sci. Rep. **6** (2016) 32501. https://doi.org/10.1038/srep32501.
30. Yuanbo Y., Pengzhan Y., Jinzhi W., Xianglian L., Zhengliang D., Yimin Ch. J. C. - Enhancing thermoelectric performance of Cu_3SnS_4-based solid solutions through coordination of the Seebeck coefficient and carrier concentration, J. Mater. Chem. A **5** (2017) 18808-18815. https://doi.org/10.1039/C7TA05253G.